Synthetic streams in a Gravitational Wave inspiral search with a multi-detector network

Haris K* and Archana Pai†
Indian Institute of Science Education and Research Thiruvananthapuram, CET Campus, Trivandrum 695016
(Dated: December 3, 2015)

Gravitational Wave Inspiral search with a global network of interferometers when carried in a phase coherent fashion would mimic an *effective* multi-detector network with synthetic streams constructed by the linear combination of the data from different detectors. For the first time, we demonstrate that the two synthetic data streams pertaining to the two polarizations of Gravitational Wave can be derived prior to the maximum-likelihood analysis in a most natural way using the technique of singular-value-decomposition applied to the network signal-to-noise ratio vector. We construct the *network matched filters* in combined network plus spectral space which capture both the synthetic streams. We further show that the network LLR is then sum of the LLR of each synthetic stream. The four extrinsic parameters namely $\{A_0, \phi_a, \epsilon, \psi\}$ are mapped to the two amplitudes and two phases namely $\{\boldsymbol{\rho}_L, \boldsymbol{\rho}_R, \Phi_L, \Phi_R\}$. The maximization over these is a straightforward approach closely linked to the single detector approach. Towards the end, we connect all the previous works related to the multi-detector Gravitational Wave inspiral search and express in the same notation in order to bring under the same footing.

PACS numbers: 04.80.Nn, 07.05.Kf, 95.55.Ym

arXiv:1401.7967v1 [gr-qc] 30 Jan 2014

I. INTRODUCTION

Global network of broad band advanced gravitational wave(GW) detectors such as Advanced LIGO, Advanced Virgo [1, 2] will be ready in next few years. Japanese detector KAGRA is under construction and would be functioning in next decade [3]. The detectors are aimed to detect few inspiral events per month from one of the prominent sources of GWs namely compact binaries with a range around 200 Mpc when GW search is carried out individually on each detector [1, 4].

The compact binary (with component masses m_1 and m_2) search through the detection of inspiral phase is carried out by phase matching technique well known as the matched filtering applied to the output data from a single detector. The signal is characterized by many physical parameters namely, for non-spinning inspiraling binaries the parameter space is $(\mathcal{M}, \eta, \mathrm{A}_0, t_a, \phi_a)$. Here, ϕ_a is the phase of the signal at the time of arrival t_a. The mass $\mathcal{M} = (m_1 m_2)^{3/5}/(m1 + m2)^{1/5}$ is the chirp mass and $\eta = m_1 m_2/(m_1 + m_2)$ is the symmetric mass ratio. A_0 is the overall amplitude. The detection is carried out by laying the templates in the multi-dimensional parameter space and then maximizing the matched filter output. This is technically known as Maximum Likelihood Ratio (MLR) analysis which is assumed to be optimal when signal-to-ratio is large and signal is buried in the noisy Gaussian data [5, 6].

In inspiral search using a multi-detector network with Advanced LIGO, Advanced Virgo etc, each interferometer is arbitrarily oriented due to its location on the globe. Thus they have different response to the incoming GW from given direction. Thus, the phase coherent detection with multi-detector network which would involve incorporating the inspiral signal from different detectors in a phase coherent fashion is a natural way to carry out multi-detector coherent analysis. Further, with this additional information from different detectors, the network removes the degeneracy of the single detector. As a result the search parameter space increases to $(\mathcal{M}, \eta, \mathrm{A}_0, t_a, \phi_a, \theta, \phi, \epsilon, \Psi)$. Where (θ, ϕ) represents the source location, ϵ is the inclination angle and Ψ is the polarization angle of the binary system. For example, two independent detectors can measure GW polarization predicted by Einstein's GR and hence the polarization becomes an explicit parameter. Similarly, at least 4 detectors are necessary to measure the source location by triangulation method[7].

The multi-detector inspiral GW search has been developed in the literature for more than a decade by various groups around the world [8–10]. In [8], the coherent formalism based on the MLR was developed and the 4 out of above mentioned 9 parameters, namely $(\mathrm{A}_0, \phi_a, \epsilon, \Psi)$ were maximized using the rotation group symmetries and Gel-Fand functions. The network likelihood ratio was shown to be sum-square of the projected network correlation function vectors on the (2-D) polarization plane. In [9], the coherent formalism was developed for a general case of correlated noise (to treat LIGO-Hanford and LIGO-Livingston). In [10], the coherent formalism was developed based on the F-statistic [11, 12], where the 4 physical parameters $(\mathrm{A}_0, \phi_a, \epsilon, \Psi)$ are mapped to the 4 amplitude parameters namely $(\mathcal{A}_1, \mathcal{A}_2, \mathcal{A}_3, \mathcal{A}_4)$. It was shown that the MLR over these parameters is equivalent to the linear least square problem. The authors showed that the freedom of polarization angle Ψ allows to set the dominant polarization frame in which the two GW

*Electronic address: haris@iisertvm.ac.in
†Electronic address: archana@iisertvm.ac.in

polarizations are separable. For more reference on the dominant polarization frame; see [13]. Finally, the authors show that the MLR analysis gives two terms which can be interpreted as the matched filtering output of the two synthetic streams constructed from the output of the multiple detectors; e.g. Eq.(2.35) of [10]. For more references on the synthetic streams in the GW burst context; see [14] and GW unmodeled chirps; see [15].

Synthetic streams would act like the building blocks for the Aperture Synthesis technique for GW search with two polarizations predicted by Einstein's GR. Aperture Synthesis is a standardized technique to combine signals from multiple telescopes for localization in electromagnetic window. This technique is used in the optical as well as in the radio telescopes where the signals are combined from distinct telescopes with the directional dependent coefficients to point to a direction. The earlier literature in inspiral search using multiple detectors [8–10] shows that the MLR in the multi-detector framework gives two synthetic data streams. The quadrature matched filtering through these synthetic data streams gives the network likelihood.

In this paper, we show that the synthetic streams is a natural way to combine the data streams in a phase coherent fashion mimicking a pair of *effective multi-detector antennas* even before the construction of MLR. This is obtained using the multi-detector singular-value-decomposition (SVD) of the *'signal-to-noise ratio (SNR) vector'* in a much more straightforward way. The highlights of the paper are as follows.

1. The singular vectors of the *network SNR vector* naturally gives the *Dominant Polarization (DP)* frame.

2. The new formalism imposes the simultaneous matched filtering in the spectral as well as network space and hence termed as *network matched filter* which give a pair of synthetic streams, which is similar to the ones obtained in earlier literatures through Maximum Likelihood Ratio(MLR).

3. The network log likelihood ratio (LLR) expressed in terms of the synthetic streams corresponding to the two singular vectors is the sum of the LLRs of the two effective synthetic data streams.

4. In this framework, the 4 physical extrinsic parameters, $(\mathrm{A}_0, \phi_a, \epsilon, \Psi)$ are mapped to four effective parameters, namely $(\boldsymbol{\rho}_L, \boldsymbol{\rho}_R, \Phi_L, \Phi_R)$.

5. The network MLR amounts to maximizing LLR over the 2 effective amplitudes $(\boldsymbol{\rho}_L, \boldsymbol{\rho}_R)$ and 2 effective phases, (Φ_L, Φ_R). This is a clear extension of the single detector data stream to analysis of two effective synthetic streams (due to multi-detector network) corresponding to two polarizations. Thus, the synthetic streams mimic the multi-detector network.

The approach gives an elegant way to obtain and construct the synthetic streams in multi-detector analysis. Further, we connect this work to all the existing works namely [8, 10] bringing different notations under the same umbrella.

The paper is organized as follows. Sec. II gives a brief outlines the binary signal with two polarizations in the multi-detector network. In Sec. III we define a SNR vector $\boldsymbol{\varrho}$ and using the singular-value decomposition technique, we show that the norm of the same which is the network SNR is the square root of the sum of the two distinct quantities, $\boldsymbol{\rho}_L^2$ and $\boldsymbol{\rho}_R^2$. In Sec. IV we obtain two synthetic streams as linear combinations of network signal such that their respective SNR's are $\boldsymbol{\rho}_L$ and $\boldsymbol{\rho}_R$. In Sec. V, we construct the network Likelihood statistic, Λ in terms of synthetic streams. Further, we show that the extrinsic physical parameters are mapped into $(\boldsymbol{\rho}_L, \boldsymbol{\rho}_R, \Phi_L, \Phi_R)$. *Thus, the network MLR analysis is equivalent to the MLR analysis of the 2 independent network synthetic streams and the maximization is equal to maximizing the 2 effective amplitudes and the 2 effective phases.* In Sec. VI we connect our results to the existing literature.

II. GW INSPIRAL BINARY SIGNAL IN A MULTI-DETECTOR NETWORK

In this section, we construct the inspiral GW signal as observed by a network of I interferometric GW antennas. The time domain restricted GW waveform (two polarizations) from a non-spinning compact binary with masses m_1, m_2 and located at a distance r which enters the interferometric detector band at time t_a with the phase ϕ_a is

$$\begin{aligned} h_+(t) &= \mathrm{A}(m_1, m_2, r, t)\frac{1+\cos^2\epsilon}{2}\,\cos\left[\Phi(t-t_a)+\phi_a\right], \\ h_\times(t) &= \mathrm{A}(m_1, m_2, r, t)\cos\epsilon\,\sin\left[\Phi(t-t_a)+\phi_a\right], \end{aligned} \quad (1)$$

where $\Phi(t-t_a)$ is the phase restricted to 3.5 PN order and the inclination angle, ϵ is the angle between orbital angular momentum vector and observer's line of sight.

The strain (response) measured by any interferometric GW detector to this GW is

$$s(t) \equiv \mathrm{F}_+\; h_+(t) + \mathrm{F}_\times\; h_\times(t)\,, \quad (2)$$

where F_+ and $\mathrm{F}_\times$ are the antenna pattern functions which describe the angular response of an antenna to a given source location. Thus, they depend on the source location with respect to the detector's site.

In a multi-detector network with I antennas at distinct locations, we represent the antenna patterns as I-dimensional vectors namely $\mathbf{F}_{+,\times} = \{\mathrm{F}_{+,\times_m}\}$ where the subscript m varies from 1 to I. In addition, different detectors receive the $h_{+,\times_m}$ with time-delays depending on the location of the detector on Earth's globe. Thus, the signal at the m-th detector site is $s_m(t) = s_{ref}(t-\tau_m)$,

where $s_{ref}(t)$ is the GW signal in the geocentric frame, which we treat as reference here and τ_m is the time delay between signal in the m-th detector and the geocentric frame with respect to source location. However, for the context of this paper, henceforth we assume that we compensate for the delays and consider the delayed signal keeping the same notation to construct the network signal[1].

The antenna pattern vectors, $\mathbf{F}_{+,\times}$ are the functions of the polarization angle Ψ, source location (θ, ϕ) and detector's Euler angles with respect to geocentric frame. We use $(\alpha_m, \beta_m, \gamma_m)$ to represent m-th detector's Euler angles following the convention in the literatures [8, 10, 15].

In the same spirit, we express the delayed and sampled signal arrived at the m-th detector with $2N$ number of time samples as a $2N$ dimensional vector,[2]

$$\mathbf{s}_m = \mathrm{F}_{+m}\ \mathbf{h}_+ + \mathrm{F}_{\times m}\ \mathbf{h}_\times \equiv \Re\left[\mathrm{F}^*_m\ \mathbf{h}\right]\,, \qquad (3)$$

where $\mathbf{h} = \mathbf{h}_+ + i\mathbf{h}_\times$ and $\mathrm{F}_m = \mathrm{F}_{+m} + i\mathrm{F}_{\times m}$ is the complex antenna pattern.

In frequency domain signal becomes,

$$\tilde{\mathbf{s}}_m = \mathrm{F}_{+m}\ \tilde{\mathbf{h}}_+ + \mathrm{F}_{\times m}\ \tilde{\mathbf{h}}_\times\,, \qquad (4)$$

where N-dimensional vectors $\tilde{\mathbf{h}}_+$ and $\tilde{\mathbf{h}}_\times$ are the discrete versions of frequency domain GW polarizations $\tilde{h}_+(f)$ and $\tilde{h}_\times(f)$ in the positive frequency region. From Eq.(1), it can be shown[3], that

$$\begin{aligned}\tilde{h}_+(f) &= \mathrm{A}_0\frac{1+\cos^2\epsilon}{2}\ h_0(f)e^{i\phi_a}\,,\\ \tilde{h}_\times(f) &= \mathrm{A}_0\cos\epsilon\ h_{\pi/2}(f)e^{i\phi_a}\,,\end{aligned} \qquad (5)$$

with $\tilde{h}_0(f) = i\tilde{h}_{\pi/2}(f) = f^{-7/6}e^{i\varphi(f)}$, the stationary phase approximated frequency domain waveform. Here A_0 is the constant which depends on the masses and the distance and $\varphi(f)$ is the 3.5 PN corrected phase of inspiral signal[17]. In the coming sections we use $\tilde{\mathbf{h}}_0$ and $\tilde{\mathbf{h}}_{\pi/2}$ to represent discrete versions of $\tilde{h}_0(f)$ and $\tilde{h}_{\pi/2}(f)$ respectively.

Thus, the incoming signal to a multi-detector network of I interferometric detectors with N number of frequency samples is expressed as a $N \times I$ matrix,

$$\tilde{\boldsymbol{\mathcal{S}}}_{N\times I}\ \equiv\ [\tilde{\mathbf{s}}_1\ \tilde{\mathbf{s}}_2\ \ldots\tilde{\mathbf{s}}_I]\,. \qquad (6)$$

[1] Note that for construction of the likelihood, this is reasonable. However, if one needs to place the templates in the directional space[16], one needs to explicitly incorporate the delays in the formalism.

[2] We take $2N$ time samples so that there would be N positive frequency samples as we work in frequency domain rest of the paper

[3] The Fourier transform is, $\tilde{G}(f) = \int_{-\infty}^{\infty} G(t)e^{-2\pi i f t}dt$.

III. NETWORK SNR

We assume that the noises in individual detectors to be independent, additive, stationary Gaussian. Thus the square of matched filter SNR of the combined network is the sum of squares of matched filter SNRs of the individual detectors [8, 10, 15] as follows,

$$\begin{aligned}\boldsymbol{\rho}^2 &= \sum_{m=1}^{I}\rho_m^2 = 4\sum_{m=1}^{I}\left[\sum_{j=1}^{N}\frac{\left|\tilde{\mathcal{S}}_{jm}\right|^2}{\mathcal{N}_{jm}}\right]\,,\\ &= \mathrm{A}_0^2\ \left[\sum_{m=1}^{I} g_m^2\mathrm{F}^2_{+m}\left(\frac{1+\cos^2\epsilon}{2}\right)^2 + g_m^2\mathrm{F}^2_{\times m}\cos^2\epsilon\right]\end{aligned} \qquad (7)$$

where, $\mathcal{N}_{jm}$ is the j-th frequency component of one sided noise power spectral density(PSD) vector of m-th antenna[4][18] and $g_m^2 = \langle\mathbf{h}_0|\mathbf{h}_0\rangle_m$ [5]. Here subscript m denotes the noise PSD of m-th detector to be used. The g_m's depict the SNR ratio in different detectors arising solely due to the noise PSD. When all the noise PSD's are identical then $g_m = g$, a constant. Note that this g_m is proportional to the one defined in [8]-Eq.(3.12).

A. Network SNR Vector

The form of $\boldsymbol{\rho}^2$ in Eq.(7) motivates us to define a I-dimensional SNR vector,

$$\boldsymbol{\varrho} \equiv \mathrm{A}_0\left[\left(\frac{1+\cos\epsilon}{2}\right)^2 e^{-2i\Psi}\quad \left(\frac{1-\cos\epsilon}{2}\right)^2 e^{2i\Psi}\right]\underbrace{\begin{bmatrix}\mathbf{d}^T\\ \\ \mathbf{d}^H\end{bmatrix}}_{\mathbf{D}^T}, \qquad (8)$$

with $\mathbf{d} \equiv \{\mathbf{F}'\exp(2i\Psi)\}$ and $\mathbf{d}^T$, $\mathbf{d}^H$ represent Transpose and Hermitian conjugate of $\mathbf{d}$ respectively, where

$$\mathrm{F}'_m = g_m\mathrm{F}_m = d_m(\theta,\phi,\alpha_m,\beta_m,\gamma_m)e^{-2i\Psi}\,, \qquad (9)$$

is the noise weighted complex antenna pattern function constructed from F_{+m}, $\mathrm{F}_{\times m}$ and g_m [6]. Further, it can be easily shown that the norm-square $\boldsymbol{\varrho}\boldsymbol{\varrho}^H$ is the network SNR square $\boldsymbol{\rho}^2$ as given in Eq.(7).

Here we use the fact that the Ψ dependence in the complex antenna pattern can be separated into a phase as given in Eq.(9). This ensures freedom in the choice of Ψ *via* the orientation of the wave frame with respect the reference frame. If we rotate the wave plane by an additional angle $\Delta\Psi$ about the line of sight(Z-axis), the network antenna pattern for this newly rotated wave frame

[4] $\mathbf{E}\left[|\tilde{n}_{jm}|^2\right] = \frac{1}{2}\mathcal{N}_{jm}$, where $\tilde{n}_{jm}$ is the j^{th} frequency component of noise in the m^{th} detector.

[5] The scalar product $\langle\mathbf{a}|\mathbf{b}\rangle_m = 4\Re\sum_{j=1}^{N}\frac{\tilde{a}_j\ \tilde{b}_j^*}{\mathcal{N}_{jm}} \equiv 4\Re\sum_{j=1}^{N}\tilde{\tilde{a}}_j\ \tilde{b}_j^*$. $\tilde{\tilde{\mathbf{a}}}$ is the frequency domain vector for the over-whitened signal $\mathbf{a}$.

[6] The vector $\mathbf{d}$ is the noise weighted version of the one defined in [15]

can be obtained by applying an equivalent transformation on $\mathbf{F}$ as, $\mathbf{F}\exp(-2i\Delta\Psi)$. That would also transform the signal as $\mathbf{h}\exp(-2i\Delta\Psi)$ keeping the response Eq.(4) invariant. This freedom in the choice of Ψ is crucial to choose appropriate frame.

We use the technique of SVD to decompose $\boldsymbol{\varrho}$ into a sum of two orthogonal vectors in the I-dimensional space. We further show below that the SVD naturally sets a particular choice for Ψ which is indeed shown to be related to the DP frame discussed in the literature.

The SVD of $\mathbf{D}$ is,

$$\mathbf{D} = \underbrace{[\hat{\mathbf{u}}_1 \quad \hat{\mathbf{u}}_2]}_{\mathbf{U}} \underbrace{\begin{bmatrix} \frac{\|\mathbf{u}_1\|}{\sqrt{2}} & 0 \\ 0 & \frac{\|\mathbf{u}_2\|}{\sqrt{2}} \end{bmatrix}}_{\Sigma} \underbrace{\frac{1}{\sqrt{2}} \begin{bmatrix} e^{i\frac{\delta}{2}} & e^{-i\frac{\delta}{2}} \\ ie^{i\frac{\delta}{2}} & -ie^{-i\frac{\delta}{2}} \end{bmatrix}}_{\mathbf{V}^H}, \quad (10)$$

where $(\mathbf{U}, \Sigma, \mathbf{V})$ have similar form as described in section IV of [15]. The columns of $\mathbf{U}$, $\hat{\mathbf{u}}_1$ and $\hat{\mathbf{u}}_2$ are the left singular vectors and those of $\mathbf{V}$ are the right singular vectors of $\mathbf{D}$. The diagonal elements of Σ are the singular values of $\mathbf{D}$.

The orthogonal pair $\{\mathbf{u}_1, \mathbf{u}_2\}$ can be written down in terms of the antenna pattern functions as

$$\mathbf{u}_1 \equiv 2\Re\left[\mathbf{F}' e^{2i\chi}\right], \qquad \mathbf{u}_2 \equiv 2\Im\left[\mathbf{F}' e^{2i\chi}\right], \quad (11)$$

with[7] $\|\mathbf{u}_{1,2}\| = \sqrt{2\left(\mathbf{d}^H\mathbf{d} \pm |\mathbf{d}^T\mathbf{d}|\right)}$ and the phase $\chi = \Psi - \frac{\delta}{4}$. The shift in Ψ, $\delta/4 = arg(\mathbf{d}^T\mathbf{d})/4$ solely depends on the multi-detector network orientation with respect to the source location. Thus, for different sky-positions, the χ would vary for a given network configuration.

Substituting back in Eq.(8), we obtain the network SNR vector as a linear combination of two orthogonal vectors

$$\begin{aligned} \boldsymbol{\varrho} &= \frac{\mathrm{A}_0}{2}\left(\frac{1+\cos^2\epsilon}{2}\cos 2\chi - i\cos\epsilon\,\sin 2\chi\right)\mathbf{u}_1^T \\ &+ \frac{\mathrm{A}_0}{2}\left(\frac{1+\cos^2\epsilon}{2}\sin 2\chi + i\cos\epsilon\,\cos 2\chi\right)\mathbf{u}_2^T. \quad (12) \end{aligned}$$

By using orthogonality property of $\mathbf{u}_1$ and $\mathbf{u}_2$, we can show that $\boldsymbol{\rho}^2$ can be written as the sum of two individual terms arising from the orthogonal vectors in the network SNR vector. Please note that unlike Eq.(7), the above equation is expressed in terms of orthogonal $\{\mathbf{u}_1, \mathbf{u}_2\}$ pair. For the sake of completeness, we give below the network SNR in terms of the individual SNRs.

$$\begin{aligned} \boldsymbol{\varrho}\boldsymbol{\varrho}^H &= \boldsymbol{\rho}_L^2 + \boldsymbol{\rho}_R^2 \\ &= \frac{\mathrm{A}_0^2\|\mathbf{u}_1\|^2}{4}\underbrace{\left[\left(\frac{1+\cos^2\epsilon}{2}\right)^2\cos^2 2\chi + \cos^2\epsilon\sin^2 2\chi\right]}_{\mathrm{P}_L^2} \\ &+ \frac{\mathrm{A}_0^2\|\mathbf{u}_2\|^2}{4}\underbrace{\left[\left(\frac{1+\cos^2\epsilon}{2}\right)^2\sin^2 2\chi + \cos^2\epsilon\cos^2 2\chi\right]}_{\mathrm{P}_R^2} \quad (13) \end{aligned}$$

[7] $\|\ .\ \|$ represents the Euclidean norm of a vector.

Here we can see that the two linear polarizations, $(+, \times)$ are linearly combined to form a pair of Left(L) and Right(R) circular polarizations. More discussion on circular polarizations is given in section IV.

This motivate us to construct two synthetic streams which would each give an individual SNR, $\boldsymbol{\rho}_L$ and $\boldsymbol{\rho}_R$. We address this in the subsequent section IV.

B. Connection to Dominant Polarization Frame

Dominant polarization(DP) frame is a specific choice of wave frame in which the the real and imaginary part of noise weighted complex network antenna pattern vector, $\mathbf{F}'^{DP} = \mathbf{F}_+'^{DP} + i\mathbf{F}_\times'^{DP}$ becomes orthogonal to each other. *i.e.*

$$\sum_{m=1}^{I} \mathrm{F}'_{+\,m}{}^{DP}\,\mathrm{F}'_{\times\,m}{}^{DP} = 0. \quad (14)$$

This is possible by a certain choice of polarization angle, Ψ^{DP} of wave frame with respect to geocentric frame . The word was coined in the context of detection of bursts by Klimenko [13] and recently in the inspiral search with multi-detector network in [10].

From Eq.(9), we can write

$$\mathbf{F}'^{DP} = \mathbf{d}\ e^{-2i\Psi^{DP}}. \quad (15)$$

Our aim is to relate Ψ^{DP} to the angles given in the SVD framework.

We note that a vector $\mathbf{F}'e^{2i\chi}$ from Eq.(11) has orthogonal real and imaginary component vectors, which is precisely the condition for antenna pattern vectors in the DP frame. Thus, the SVD provides a natural connection to the DP frame through its construction.

In summary,

$$\begin{aligned} \mathbf{F}'^{DP} &= \mathbf{F}'e^{2i\chi} = \frac{\mathbf{u}_1 + i\mathbf{u}_2}{2} = \mathbf{d}e^{-i\frac{\delta}{2}}, \\ \mathbf{F}_+'^{DP} &= \frac{\mathbf{u}_1}{2} \quad \text{and} \quad \mathbf{F}_\times'^{DP} = \frac{\mathbf{u}_2}{2}, \quad (16) \end{aligned}$$

and $\Psi^{DP} = \delta/4$. The DP frame is obtained by rotating wave frame about z-axis by an angle $\chi = \Psi - \delta/4$ in clockwise direction. As is expected, the DP frame is pertaining to a source; *i. e.* with the change in the location of the source, the χ (the angle through which one needs to rotate to bring into the DP frame) would change.

IV. APERTURE SYNTHESIS IN GW INSPIRAL SEARCH

As mentioned earlier, more than one detector is necessary to determine GW polarization as well as localization of the sources [19]. In the following discussion, we construct two effective synthetic data streams out of I detector data streams in the network, they together carry

full network SNR as given in Eq.(7). Since GW carry two polarizations in the Einsteinian GR, the signal resides in the 2-dimensional sub-space of I-dimensional network space and hence only two independent data streams are sufficient to provide information about the polarization in the network formalism. We show that the constructed data streams provide that information. In the past [8, 10, 15], the synthetic data streams were shown to be the by-product of maximizing the network LLR over the four extrinsic parameters $(A, \phi_a, \epsilon, \Psi)$. However, here in this section, we show that the synthetic streams can be constructed prior to the MLR analysis. This is similar to the spirit of aperture synthesis technique in the electromagnetic window such as optical or radio used in Very Large Telescope Interferometer(VLTI) or Very Long Baseline Interferometry (VLBI) , where an effective antenna is constructed out of linear combination of data from different telescopes.

First, we construct the synthetic data streams using $\mathbf{u}_1$ and $\mathbf{u}_2$ and show that they individually give the matched filter SNR equal to $\boldsymbol{\rho}_L$ and $\boldsymbol{\rho}_R$.

A. Signal $\mathbf{s}_m$ in the DP Frame

In the rest of the paper, we work in the new frame provided by the SVD *aka* the DP frame. We first rewrite the antenna pattern $\mathbf{F}$ in terms of $\mathbf{u}_1$ and $\mathbf{u}_2$, and then express the network signal in time as well as frequency domain as below.

Using Eq.(3) and Eq.(16), the time domain signal vector at m-th detector is

$$\begin{aligned}\mathbf{s}_m &= \frac{1}{2}\,\Re\left[\mathbf{h}\; e^{2i\chi}\;\frac{u_{1m}}{g_m}\right] + \frac{1}{2}\,\Im\left[\mathbf{h} e^{2i\chi}\;\frac{u_{2m}}{g_m}\right], \\ &= \Re\left[\mathbf{h}\; e^{2i\chi}\;\left(\frac{u_{1m}+iu_{2m}}{2g_m}\right)^*\right] \equiv \Re[\mathbf{h}^{DP}\;\mathbf{F}_m^{DP*}] \quad (17)\end{aligned}$$

where $\mathbf{h}^{DP} = \mathbf{h}\exp(2i\chi)$ and $\mathbf{F}^{DP} = \mathbf{F}\exp(2i\chi)$ are the complex GW as well as the network antenna pattern function in the DP frame respectively.

In frequency domain, the j-th frequency component of the signal in m-th detector, $[\tilde{\mathbf{s}}_m]_j = \tilde{\mathcal{S}}_{jm}$ can be expressed in terms of linear combination of $\mathbf{F}^{DP}_{+,\times}$ in the DP frame. Further, the amplitude A_0, initial phase ϕ_a and frequency dependent part namely $\tilde{\mathbf{h}}_0$ are factored out as shown below

$$\begin{aligned}\tilde{\mathcal{S}}_{jm} &= \mathrm{A}_0 e^{i\phi_a}\tilde{h}_{0j}\left[\left(\frac{1+\cos^2\epsilon}{2}\;\cos 2\chi + i\cos\epsilon\;\sin 2\chi\right)\mathrm{F}^{DP}_{+m}\right. \\ &\quad \left. + \left(\frac{1+\cos^2\epsilon}{2}\;\sin 2\chi - i\cos\epsilon\;\cos 2\chi\right)\mathrm{F}^{DP}_{\times m}\right] \\ &\equiv \mathrm{A}_0\tilde{h}_{0j}\left[\mathrm{P}_L\,\mathrm{F}^{DP}_{+m}\,e^{i\Phi_L} + \mathrm{P}_R\,\mathrm{F}^{DP}_{\times m}\,e^{i\Phi_R}\right]. \quad (18)\end{aligned}$$

The $\mathrm{P}_{L,R}$ are the polarization amplitudes in the DP frame as defined in Eq.(13). This carry the effect of rotation by 2χ of the signal which mixes the two linear GW polarizations into a pair of *left(L) and right(R) Circular Polarizations*. The polarization phases are,

$$\begin{aligned}\Phi_L(\epsilon,\chi) &= \tan^{-1}\left[\tan(2\chi)\;\;\frac{2\cos\epsilon}{1+\cos^2\epsilon}\right] + \phi_a, \quad (19)\\ \Phi_R(\epsilon,\chi) &= \Phi_L\left(\epsilon, \chi+\frac{\pi}{4}\right). \quad (20)\end{aligned}$$

As expected the Φ_R phase is obtained by rotating χ by $\pi/4$ in Φ_L; the property of GW polarizations. The above polarization terms; namely $\{\mathrm{P}_{L,R}e^{i\Phi_{L,R}}\}$ can be shown to be equal to

$$\begin{aligned}\mathrm{P}_L e^{i\Phi_L} &= \left[T^*_{2+2}(\chi,\epsilon,0) + T^*_{2-2}(\chi,\epsilon,0)\right] \quad (21)\\ \mathrm{P}_R e^{i\Phi_R} &= i\left[T^*_{2-2}(\chi,\epsilon,0) - T^*_{2+2}(\chi,\epsilon,0)\right] \quad (22)\end{aligned}$$

respectively, which describe the circular polarizations expressed in terms of rank-2 Gel-Fand function T_{mn} [22] [8].

In the next subsection, we use this separation feature of the signal to construct the synthetic streams.

B. Network Matched Filter

In this section, we introduce the notion of a matched filter designed for a the multi-detector analysis which not only combines the spectral but also the network features. We call this filter as the *network matched filter*.

Let the frequency domain delayed network data stream is given by $\tilde{\boldsymbol{\mathcal{X}}} = [\tilde{\mathbf{x}}_1\;\tilde{\mathbf{x}}_2 \ldots \tilde{\mathbf{x}}_I]$ with $\tilde{\mathbf{x}}_m = \tilde{\mathbf{s}}_m + \tilde{\mathbf{n}}_m$ and $\tilde{\mathbf{n}}_m$ is the frequency domain noise vector corresponding to m-th detector. To proceed further, we make following constructs.

1. *Over-whitened data stream*: Construct over-whitened data stream incorporating the noise PSD of the individual antennas denoted by $\tilde{\tilde{\mathcal{X}}}_{jm} = \frac{\tilde{\mathcal{X}}_{jm}}{\mathcal{N}_{jm}}$.

2. *Synthetic data stream*: The over-whitened synthetic data stream $\tilde{\tilde{\mathbf{z}}}$ is constructed from the linear combination of individual over-whitened data streams as below,

$$\tilde{\tilde{z}}_j \equiv \sum_{m=1}^{I}\alpha_m\tilde{\tilde{\mathcal{X}}}_{jm}, \quad (23)$$

with real linear coefficients α_m. The over-whitened data is used for the synthetic data stream construction in order to incorporate the individual noise PSDs.

---

[8] The rank-2 Gel-Fand functions

$$T^2_{2\pm2}(\chi,\epsilon,0) = \frac{(1\pm\cos\epsilon)^2}{4}\exp(\mp 2i\chi).$$

Since throughout the paper we use only rank-2 Gel-Fand functions, we drop the superscript 2 from T^2_{mn}.

We show in the rest of the section that using the classical idea of matched filtering, we can tune α_m such that the resulting synthetic data stream would observe either $left$(L) or $right$(R) circular polarization.

In the next subsection, we remind the reader the classical derivation of the matched filter used for the single detector context.

1. Single Detector Matched Filter

If $\tilde{\mathbf{k}}$ is a filter, then the filtered output of $\tilde{\mathbf{z}}$ through this filter is $\langle \mathbf{z} \mid \mathbf{k} \rangle$. Here, (in order to avoid the excess notations) for this sub-subsection, let us assume that $\tilde{\mathbf{z}}$ denotes the un-whitened data of the single detector.

The SNR of the filtered output is [23],

$$\text{SNR} \;=\; \frac{\mathbf{E}\left[\langle \mathbf{z} \mid \mathbf{k} \rangle\right]}{\boldsymbol{\sigma}\left[\langle \mathbf{z} \mid \mathbf{k} \rangle\right]|_{\tilde{\boldsymbol{s}}=0}} = \frac{4\Re\left[\sum_{j=1}^{N} \mathrm{E}\left(\tilde{\tilde{s}}_j \tilde{k^*}_j\right)\right]}{\sqrt{\mathrm{E}\left[\left(4\Re\left[\sum_{l=1}^{N} \tilde{\tilde{s}}_l \tilde{k}_l^*\right]\right)^2\right]\Big|_{\tilde{\boldsymbol{s}}=0}}}, \tag{24}$$

where $\mathbf{E}[\,.\,]$ represents the expectation and $\boldsymbol{\sigma}[\,.\,]$ represents the standard deviation. The single detector SNR further simplifies to

$$\text{Single detector SNR} = \frac{4\Re\left[\sum_{j=1}^{N} \tilde{\tilde{s}}_j \; \tilde{k}_j^*\right]}{\sqrt{4 \; \sum_{j=1}^{N} \frac{\left|\tilde{k}_j\right|^2}{\mathcal{N}_j}}} = \langle \mathbf{s} | \hat{\mathbf{k}} \rangle. \tag{25}$$

The filter norm is $\sqrt{\langle \mathbf{k} | \mathbf{k} \rangle}$. As is known, the above SNR would be optimal when the filter vector is aligned to the signal vector *i.e.* $\tilde{k}_j \propto \tilde{s}_j$ known as the matched filter.

Now, let us explore these ideas in the context of the multi-detector scenario.

2. Network Matched Filter

The matched filter is that filter which gives the optimum SNR in Gaussian noise. However, the signal in DP frame is separated in such a way that the noise weighted antenna patterns are orthogonal. Let us apply the matched filter notion with the aim that the resultant combined spectral as well as network filter *via* α_m would capture the individual polarizations. We show below that in this exercise, this amounts to constructing a combined matched filter.

Consider Eq.(24) with $\tilde{\mathbf{z}}$ as the synthetic stream defined in Eq.(23). Then, Eq.(24) can be simplified to

$$\text{SNR} = \frac{4\Re\left[\sum_{j=1}^{N}\sum_{m=1}^{I} \tilde{\tilde{\mathcal{S}}}_{jm} \tilde{\mathcal{K}}^*_{jm}\right]}{\sqrt{4 \; \sum_{j=1}^{N}\sum_{m=1}^{I} \frac{\left|\tilde{\mathcal{K}}_{jm}\right|^2}{\mathcal{N}_{jm}}}} \;, \tag{26}$$

where $\tilde{\boldsymbol{\mathcal{K}}} = \tilde{\mathbf{k}} \otimes \boldsymbol{\alpha}$. *i.e.* $\tilde{\mathcal{K}}_{jm} = \tilde{k}_j \alpha_m$ and $\tilde{\mathcal{K}}_m = \alpha_m \tilde{\mathbf{k}}$.

Further The denominator of Eq.(26),

$$\sqrt{4 \; \sum_{j=1}^{N}\sum_{m=1}^{I} \frac{\left|\tilde{\mathcal{K}}_{jm}\right|^2}{\mathcal{N}_{jm}}} = \sum_{m=1}^{I} \alpha_m^2 \langle \mathbf{k} | \mathbf{k} \rangle_m^2 \tag{27}$$

is the Frobeinus matrix norm of $\tilde{\mathcal{K}}_{\mathbf{N}\times\mathbf{I}}$ in the combined spectral-network $(N \times I)$ space defined as $||\tilde{\mathcal{K}}||^2 \equiv \mathrm{Tr}(\langle \tilde{\mathcal{K}_m}, \tilde{\mathcal{K}_n} \rangle)$ which is same as the right hand side of Eq.(27). The subscript m in $\langle \mathbf{k} | \mathbf{k} \rangle_m$ denotes the noise PSD is that of m-th detector.

It is interesting to note that, Eq.(26) has the same structure of a conventional single detector matched filter SNR in the Eq.(25). For a single detector, filter is a one dimensional vector in the spectral direction. As the matched filter is that filter which gives maximum SNR, which should be aligned along the signal *i.e.* $\tilde{k}_j \propto \tilde{s}_j$ for single detector case.

While in the multi-detector case, $\tilde{\boldsymbol{\mathcal{K}}}$ is a 2-dimensional $(N \times I)$ combined spectral-network filter. Since $\tilde{\boldsymbol{\mathcal{S}}}$ can be decomposed into frequency and network components, the optimal combined filter should *match* with $\tilde{\boldsymbol{\mathcal{S}}}$ (or part of $\tilde{\boldsymbol{\mathcal{S}}}$) in the same spirit as that of the single detector case described above. Owing to the fact that detailed in Eq.(18), we recall that the network signal has two constituent parts. Here, we construct that filter which captures either of the two circular polarizations as shown below.

1. **$\tilde{\boldsymbol{\mathcal{K}}}_L$: Network Matched Filter for Left Circular polarization**
   To capture the plus polarization of DP frame ($Left$ circular polarization) in Eq.(18), $\tilde{\boldsymbol{\mathcal{K}}}_L$ should be aligned to the $Left$ polarization part of the $\tilde{\boldsymbol{\mathcal{S}}}$ which we call $\tilde{\boldsymbol{\mathcal{K}}}_L \equiv \tilde{\mathbf{k}}_L \otimes \boldsymbol{\alpha}_L$. The alignment condition demands that it should satisfy

   $$\tilde{k}_{L,j} \propto \tilde{h}_{0j} e^{i\Phi_L} \quad \text{and} \quad \alpha_{L,m} \propto \mathrm{F}^{DP}_{+m} \,. \tag{28}$$

   together. Since the Frobeinus *norm* of $\tilde{\boldsymbol{\mathcal{K}}}_L$ is $\|\mathbf{F}'^{DP}_{+}\|$, the components of normalized network plus filter $\tilde{\boldsymbol{\mathcal{K}}}_L$ become,

   $$\tilde{k}_{L,j} = \tilde{h}_{0j} e^{i\Phi_L} \;, \qquad \alpha_{L,m} = \frac{\mathrm{F}^{DP}_{+m}}{\|\mathbf{F}'^{DP}_{+}\|} \;, \tag{29}$$

   Using Eq.(26) and Eq.(29), the corresponding SNR becomes,

   $$4\Re\left[\sum_{j=1}^{N}\sum_{m=1}^{I} \tilde{\tilde{\mathcal{S}}}_{jm} \; \tilde{\mathcal{K}}_{L,jm}\right] = \boldsymbol{\rho}_L \;. \tag{30}$$

2. **$\tilde{\boldsymbol{\mathcal{K}}}_R$: Network Matched Filter for Right Circular polarization**:
   To capture the cross polarization of DP frame

(*Right* circular polarization) in Eq.(18), we construct another filter, $\tilde{\boldsymbol{\mathcal{K}}}_R \equiv \tilde{\mathbf{k}}_R \otimes \boldsymbol{\alpha}_R$ such that together it should satisfy

$$\tilde{k}_{R,j} \propto \tilde{h}_{0j} e^{i\Phi_R} \quad \text{and} \quad \alpha_{R,m} \propto \mathrm{F}^{DP}_{\times m} . \tag{31}$$

The Frobeinus norm of $\tilde{\boldsymbol{\mathcal{K}}}_R$ is $\|\mathbf{F}'^{DP}_{\times}\|$, gives the components of normalized network cross filter $\tilde{\boldsymbol{\mathcal{K}}}_R$,

$$\tilde{k}_{R,j} = \tilde{h}_{0j} e^{i\Phi_R} , \qquad \alpha_{R,m} = \frac{\mathrm{F}^{DP}_{\times m}}{\|\mathbf{F}'^{DP}_{\times}\|} . \tag{32}$$

with the corresponding SNR as given by,

$$4\Re \left[\sum_{j=1}^{N} \sum_{m=1}^{I} \tilde{\tilde{\mathcal{S}}}_{jm} \, \tilde{\mathcal{K}}_{R,jm} \right] = \boldsymbol{\rho}_R . \tag{33}$$

In summary, the synthetic streams constructed from the over-whitened data streams which captures the individual polarizations in the DP frame are

$$\tilde{\tilde{\mathbf{z}}}_L = \sum_{m=1}^{I} \frac{\mathrm{F}^{DP}_{+m}}{\|\mathbf{F}'^{DP}_{+}\|} \tilde{\tilde{X}}_{jm}, \quad \tilde{\tilde{\mathbf{z}}}_R = \sum_{m=1}^{I} \frac{\mathrm{F}^{DP}_{\times m}}{\|\mathbf{F}'^{DP}_{\times}\|} \tilde{\tilde{X}}_{jm} , \tag{34}$$

They together give the total network SNR as the sum squares of individual SNRs. The total signal power in the individual detectors of the network is now distributed among the synthetic streams $\tilde{\mathbf{z}}_L$ and $\tilde{\mathbf{z}}_R$, which when processed with filters $\tilde{\mathbf{k}}_L$ and $\tilde{\mathbf{k}}_R$ independently captures the two polarizations in DP frame. By using Eq.(29), Eq.(30), Eq.(32) and Eq.(33), we can write the respective SNRs as,

$$\boldsymbol{\rho}_L = \langle \mathbf{z}_L | \mathbf{k}_L \rangle |_{\mathbf{n}=0} , \qquad \boldsymbol{\rho}_R = \langle \mathbf{z}_R | \mathbf{k}_R \rangle |_{\mathbf{n}=0} . \tag{35}$$

Thus, we have shown that extending the concept of the matched filter to the network gives us two effective synthetic data streams which can be further processed.

C. Special Case: Same Noise for all Detectors

In this subsection, we consider an idealistic situation where all the detectors have same noise PSD, *i.e.* g_m's becomes equal to a constant 'g' for all detectors. Then from Eq.(34), we can see that the 'noise free' synthetic streams, $\tilde{\mathbf{z}}^s_{L,R}$ are nothing but the projections of network signal matrix $\tilde{\boldsymbol{\mathcal{S}}}$ on the orthonormal vectors $\hat{\mathbf{F}}^{DP}_{+,\times}$ with an over all weight $1/g$. If we expand $\tilde{\boldsymbol{\mathcal{S}}}$ as in Eq.(18), we can further simplify $\tilde{\mathbf{z}}^s_{L,R}$ into linear combination of GW polarizations, $\tilde{\mathbf{h}}_{+,\times}$ similar to a pair of ordinary interferometric detector signals as shown below.

$$\begin{aligned} \tilde{\mathbf{z}}^s_L &= \frac{\|\mathbf{F}^{DP}_{+}\|}{g} \left(\tilde{\mathbf{h}}_+ \, \cos 2\chi \, - \, \tilde{\mathbf{h}}_\times \, \sin 2\chi \right) , \\ \tilde{\mathbf{z}}^s_R &= \frac{\|\mathbf{F}^{DP}_{\times}\|}{g} \left(\tilde{\mathbf{h}}_+ \, \sin 2\chi \, + \, \tilde{\mathbf{h}}_\times \, \cos 2\chi \right) . \end{aligned} \tag{36}$$

Please note the equivalent antenna pattern of $\tilde{\mathbf{z}}^s_R$ is $\pi/4$ out of phase with that of $\tilde{\mathbf{z}}^s_L$.

V. MULTI-DETECTOR MAXIMUM LIKELIHOOD RATIO AND NETWORK SYNTHETIC STREAMS

In this section, we carry out MLR analysis for the inspiral detection with a multi-detector network. This has been already done in the literatures [8, 10, 15] in different contexts as well as notations. Here, we construct MLR statistic in much more straightforward way and latter we make connection to the previous works and thus bring all earlier multi-detector inspiral related search formalisms under the same notations.

In multi-detector network MLR detection technique,the network LLR is maximized over signal parameters and a test statistic is obtained, which is then compared with the threshold for the detection. For high SNR cases, MLR technique is known to be optimal.

A. Network Likelihood Ratio

Assuming the Gaussian, additive noise in each detector data, the LLR for a multi-detector network with I constituent detectors is the sum of LLR's of individual antennas and is given by [10],

$$\Lambda = \sum_{m=1}^{I} \langle \mathbf{x}_m | \mathbf{s}_m \rangle - \frac{1}{2} \langle \mathbf{s}_m | \mathbf{s}_m \rangle . \tag{37}$$

Re-arranging terms and little algebra as given in Appendix-A, we can re-express the above equation in terms of the synthetic data streams as

$$2\Lambda = \left[2\boldsymbol{\rho_L} \langle \mathbf{z}_L | \mathbf{h}_0 e^{i\Phi_L} \rangle - \boldsymbol{\rho}^2_{\boldsymbol{L}} \right] + \left[2\boldsymbol{\rho_R} \langle \mathbf{z}_R | \mathbf{h}_0 e^{i\Phi_R} \rangle - \boldsymbol{\rho}^2_{\boldsymbol{R}} \right] . \tag{38}$$

We note that Eq.(38) can be viewed as the sum of LLR of 2 independent synthetic detectors, where $\Phi_{L,R}$ carries the constant phase which incorporates the initial phase plus the polarization angles and $\boldsymbol{\rho}_{L,R}$ are the SNRs of the two synthetic data streams.

We note that in terms of synthetic streams, the four extrinsic parameters $(\mathrm{A}_0, \phi_a, \epsilon, \Psi)$ are now mapped in to a set of two effective SNRs and 2 effective phases, namely $(\boldsymbol{\rho}_L, \boldsymbol{\rho}_R, \Phi_L, \Phi_R)$.

B. Maximization of Network LLR

Now we maximize Λ over the new extrinsic parameters $(\boldsymbol{\rho}_L, \boldsymbol{\rho}_R, \Phi_L, \Phi_R)$ to obtain MLR $\hat{\Lambda}$ [8, 10, 15]. The new extrinsic parameters give the re-parametrized physical parameters $(\mathrm{A}_0, \phi_a, \epsilon, \Psi)$ where the relation between them is summarized in Appendix-B. Below, we maximize Λ over the new set; first over the amplitudes and then over the phase respectively.

1. **Amplitude Maximization**
   Maximization over $\boldsymbol{\rho}_{L,R}$ is same as that in case of single detector[6] and it results in,

$$2\hat{\Lambda} \mid_{\boldsymbol{\rho}_L,\boldsymbol{\rho}_R} = \langle \mathbf{z}_L|\mathbf{h}_0 e^{i\Phi_L}\rangle^2 + \langle \mathbf{z}_R|\mathbf{h}_0 e^{i\Phi_R}\rangle^2 \ , \qquad (39)$$

   and the MLR amplitude estimates become

$$\hat{\boldsymbol{\rho}}_L = \langle \mathbf{z}_L|\mathbf{h}_0 e^{i\Phi_L}\rangle \ , \qquad \hat{\boldsymbol{\rho}}_R = \langle \mathbf{z}_R|\mathbf{h}_0 e^{i\Phi_R}\rangle. \qquad (40)$$

2. **Phase Maximization**
   Since Φ_L and Φ_R are independent, maximization of LLR over them amounts to individually maximizing each term of the sum in Eq.(39). Thus the ML estimates of $\Phi_{L,R}$ are,

$$\hat{\Phi}_L = arg\left[\sum_{j=1}^{N} \tilde{\tilde{z}}_{L,j}\ \tilde{h}^*_{0j}\right] \ , \quad \hat{\Phi}_R = arg\left[\sum_{j=1}^{N} \tilde{\tilde{z}}_{R,j}\ \tilde{h}^*_{0j}\right]. \quad (41)$$

In summary,

$$2\hat{\Lambda} = 16\left[\left|\sum_{j=1}^{N} \tilde{\tilde{z}}_{L,j}\ \tilde{h}^*_{0j}\right|^2 + \left|\sum_{j=1}^{N} \tilde{\tilde{z}}_{R,j}\ \tilde{h}^*_{0j}\right|^2\right] \ . \qquad (42)$$

We write one individual term in Eq.(42) as follows,

$$\begin{aligned}
&\left|\sum_{j=1}^{N} \tilde{\tilde{z}}_{L,R\ j}\ \tilde{h}^*_{0j}\right|^2 \\
&= \left(\Re\left[\sum_{j=1}^{N} \tilde{\tilde{z}}_{L,R\ j}\tilde{h}^*_{0j}\right]\right)^2 + \left(\Re\left[\sum_{j=1}^{N} \tilde{\tilde{z}}_{L,R\ j}\tilde{h}^*_{\pi/2j}\right]\right)^2 , \\
&= \frac{\langle \mathbf{z}_{L,R}|\mathbf{h}_0\rangle^2 + \langle \mathbf{z}_{L,R}|\mathbf{h}_{\pi/2}\rangle^2}{16}. \qquad (43)
\end{aligned}$$

Thus the MLR simplifies to

$$2\hat{\Lambda} = \langle \mathbf{z}_L|\mathbf{h}_0\rangle^2 + \langle \mathbf{z}_L|\mathbf{h}_{\pi/2}\rangle^2 + \langle \mathbf{z}_R|\mathbf{h}_0\rangle^2 + \langle \mathbf{z}_R|\mathbf{h}_{\pi/2}\rangle^2. \qquad (44)$$

This can be described as quadrature sum of powers in synthetic streams $\tilde{\mathbf{z}}_L$ and $\tilde{\mathbf{z}}_R$. This is similar to the single detector statistic which contains the quadrature sum of powers in a single detector data stream. From Eq.(35) and Eq.(42), we can see under no noise condition[8, 10, 15],

$$2\hat{\Lambda} = \boldsymbol{\rho}_{\boldsymbol{L}}^2 + \boldsymbol{\rho}_{\boldsymbol{R}}^2 \ . \qquad (45)$$

VI. CONNECTION TO THE EXISTING LITERATURE

In the GW multi-detector inspiral search, network MLR statistics maximized over 4 extrinsic parameters has been formalized in the literature [8, 10]. Though the problem is same, the parametrization depends on the way the problem is casted. However, the final MLR , maximized over the extrinsic parameters is the same. In this section, we carry out comparison between various formalisms under the same notations as given here, which till now is not been done in the literature so far.

A. Synthetic Streams and Harry-Fairhurst [10] Approach

In [10], the authors casted the multi-detector MLR problem into the F-statistic. The polarizations were written down in terms of the linear combination of the 4 amplitudes on which the extrinsic parameters are mapped *i.e.*

$$(A_0, \phi_a, \epsilon, \Psi) \Rightarrow (\mathcal{A}_1, \mathcal{A}_2, \mathcal{A}_3, \mathcal{A}_4) \ . \qquad (46)$$

For explicit relations, please visit Appendix-B. Latter they transform wave frame to DP frame so that Maximum Likelihood SNR square, $2\hat{\Lambda}$ is simplified to quadrature sum of powers in + and × polarizations. Here, the maximization over the four amplitudes is carried out at a time.

Below, we derive the multi-detector MLR of [10] Eq. (2.33) starting from the notations in this paper.

In Eq.(39),

$$\begin{aligned}
\langle \mathbf{z}_{L,R}|\mathbf{h}_0\rangle &= \frac{4}{\|\mathbf{F}'^{DP}_{+,\times}\|}\Re\left[\sum_{j=1}^{N}\sum_{m=1}^{I} \tilde{\tilde{X}}_{jm}\ h_{0j}{}^*\mathrm{F}^{DP}_{+,\times m}\right] \\
&= \frac{1}{\|\mathbf{F}'^{DP}_{+,\times}\|}\sum_{m=1}^{I}\langle \mathbf{x}_m|\mathbf{h}_0\mathrm{F}^{DP}_{+,\times m}\rangle \ , \\
\text{and } \langle \mathbf{z}_{L,R}|\mathbf{h}_{\pi/2}\rangle &= \frac{1}{\|\mathbf{F}'^{DP}_{+,\times}\|}\sum_{m=1}^{I}\langle \mathbf{x}_m|\mathbf{h}_{\pi/2}\mathrm{F}^{DP}_{+,\times m}\rangle. \qquad (47)
\end{aligned}$$

Further,

$$\|\mathbf{F}'^{DP}_{+,\times}\|^2 = \sum_{m=1}^{I} g_m^2\mathrm{F}^2_{+,\times m} = \sum_{m=1}^{I}\langle \mathbf{h}_0\mathrm{F}_{+,\times m}|\mathbf{h}_0\mathrm{F}_{+,\times m}\rangle \ .$$

Now substituting back in Eq.(44),

$$\begin{aligned}
2\hat{\Lambda} &= \frac{\left[\sum_m\langle \mathbf{x}_m|\mathbf{h}_0\mathrm{F}^{DP}_{+m}\rangle\right]^2 + \left[\sum_m\langle \mathbf{x}_m|\mathbf{h}_0\mathrm{F}^{DP}_{+m}\rangle\right]^2}{\sum_m\langle \mathbf{h}_0\mathrm{F}_{+m}|\mathbf{h}_0\mathrm{F}_{+m}\rangle} \\
&+ \frac{\left[\sum_m\langle \mathbf{x}_m|\mathbf{h}_0\mathrm{F}^{DP}_{\times m}\rangle\right]^2 + \left[\sum_m\langle \mathbf{x}_m|\mathbf{h}_0\mathrm{F}^{DP}_{\times m}\rangle\right]^2}{\sum_m\langle \mathbf{h}_0\mathrm{F}_{\times m}|\mathbf{h}_0\mathrm{F}_{\times m}\rangle} \ . \qquad (48)
\end{aligned}$$

Absorbing the summation over m following the definition Eq.(2.21) of [10], Eq.(48) would go to Eq.(2.33) of [10] [9]. Also one can show that $\tilde{\tilde{\mathbf{z}}}_{L,R}$ are related to over-whitened synthetic streams $o_{+,\times}$ defined in Eq.(2.35) of [10] as follows,

$$o_{+,\times} = \|\mathbf{F}'^{DP}_{+,\times}\|\ \tilde{\tilde{\mathbf{z}}}_{L,R}. \qquad (49)$$

[9] $\langle \mathbf{a}|\mathbf{b}\rangle$ is same as $(\mathbf{a}|\mathbf{b})$ defined in Eq.(2.17) of [10].

The two pairs of synthetic streams differ by constants which is different for both the synthetic streams. The final multi-detector MLR matches to Eq. (44) as expected.

B. Synthetic Streams and Pai et al [8] Approach

In [8], the multi-detector coherent statistic was obtained by successive maximization of amplitude A_0, initial phase ϕ_a similar to single detector statistic. The polarization angles (ϵ, ψ) are maximized at a time using the symmetry properties of the rotation group and Gel-Fand functions. The MLR thus obtained contains the sum square of four terms as is shown in Eq.(4.11) of [8] similar to Eq.(2.33) of [10] and Eq.(44) above. We explicitly give the Eq.(4.11) of [8] below.

$$\begin{aligned} 2\hat{\Lambda} &= |\hat{\mathsf{v}}^+ \cdot \mathsf{C}|^2 + |\hat{\mathsf{v}}^+ \cdot \mathsf{C}|^2 \\ &= (c_0^+)^2 + (c_{\pi/2}^+)^2 + (c_0^-)^2 + (c_{\pi/2}^-)^2 \end{aligned} \tag{50}$$

where the elements of I-dimensional complex vector C,

$$C^m = c_0^m + i c_{\pi/2}^m \tag{51}$$

combines the correlations of the two quadratures of the normalized template with the data with $c_0^m = \langle \mathbf{h}_0^m | \mathbf{x}^m \rangle_{(I)}$ and $c_{\pi/2}^m = \langle \mathbf{h}_{\pi/2}^m | \mathbf{x}^m \rangle_{(m)}$. Further,

$$\hat{\mathsf{v}}^{\pm} = \frac{\mathsf{v}^{\pm}}{\|\mathsf{v}^{\pm}\|} = \frac{\widehat{\Re(\mathbf{d})} \pm \widehat{\Im(\mathbf{d})}}{\| \left(\widehat{\Re(\mathbf{d})} \pm \widehat{\Im(\mathbf{d})}\right) \|} \tag{52}$$

is a pair of real unit vectors which span the 2-dimensional polarization plane in the I-dimensional space. Thus, if we take a representative individual term in Eq.(50), it becomes

$$(c_0^+)^2 = \left(\sum_{I=m}^{I} \frac{\mathsf{v}_m^+}{\| \mathsf{v} \|} \langle \mathbf{x}_m, \mathbf{h}_0 \rangle \right)^2 \equiv \langle \mathbf{z}_+ | \mathbf{h}_0 \rangle^2 \tag{53}$$

Thus, based on Eq.(53) the corresponding synthetic streams are

$$\tilde{\tilde{\mathbf{z}}}_{+j} \equiv \sum_{m=1}^{I} \frac{\mathsf{v}_m^+}{g_m \|\mathsf{v}^+\|} \tilde{\tilde{X}}_{jm}, \quad \tilde{\tilde{\mathbf{z}}}_{-j} \equiv \sum_{m=1}^{I} \frac{\mathsf{v}_m^-}{g_m \|\mathsf{v}^-\|} \tilde{\tilde{X}}_{jm}. \tag{54}$$

which give the SNR's ρ_+ and ρ_- such that in no noise case,

$$2\hat{\Lambda} = \rho_+^2 + \rho_-^2. \tag{55}$$

C. SNRs in two pairs of Synthetic Data Streams

In this section, we explicitly show that the two data streams namely; $\tilde{\mathbf{z}}_{L,R}$ and $\tilde{\mathbf{z}}_{+,-}$ are not same though they give the same network SNR when combined in pairs.

Following Eq.(34) and Eq.(54), the two pairs of synthetic streams are constructed using a pair of two real vectors namely; $\{\mathbf{F}_{+,\times}^{\prime DP}\}$ and $\{\mathsf{v}_{\pm}\}$ respectively. We write down these real vectors explicitly in terms of $\mathbf{d}$ as,

$$\mathbf{F}_+^{\prime DP} = \Re[\mathbf{d} e^{-i\frac{\delta}{2}}], \qquad \mathbf{F}_\times^{\prime DP} = \Im[\mathbf{d} e^{-i\frac{\delta}{2}}], \tag{56}$$

$$\mathsf{v}_+ = \Re[\mathbf{d} e^{-i\alpha}], \qquad \mathsf{v}_- = \Re[\mathbf{d} e^{i\alpha}], \tag{57}$$

with $\alpha = \frac{1}{2}\cos^{-1}\left[-\frac{|\mathbf{d}^{\mathrm{T}}\mathbf{d}|\cos\delta}{\mathbf{d}^{\mathrm{H}}\mathbf{d}}\right]$ and $\delta = \arg(\mathbf{d}^T\mathbf{d})$ as defined earlier.

The figures, Fig. 1, 2, 3 are the contour plots of SNR squares of the individual synthetic data streams as well as the network SNR square as a function of the source location for a given polarization in various combinations of 3 detector networks, 4 detector networks and 5 detector network respectively. We assume all the detectors with "zero-detuning, high power" Advanced LIGO noise curve given by Eq.(4.7) of [24]. We took the binary system with component masses of $(1.4, 1.4)M_\odot$ located at the distance of 150 Mpc as source with $\epsilon = \psi = \pi/4$. We consider networks constructed out of LIGO-Livingston(L), LIGO-Hanford(H), Virgo(V), proposed KAGRA(K) and detector in India denoted by (I)[10].

Several distinct features are to be noted in the SNR figures of the two pairs; namely there is definite symmetry in the SNR pattern $\rho_{L,R}^2$ whereas $\rho_\pm^2$ lacks that feature. Further, on average network SNR seemed to have distributed between the ρ_+ and ρ_- equally whereas ρ_L carries large fraction of the network SNR. Some of these features can be used to construct consistency test for the targeted directional search which is under consideration.

VII. CONCLUSION

The multi-detector interferometric GW network can be described as a pair *effective* multi-detector antennas which captures most of the features of many detectors acting in phase coherent fashion. Till now, in the compact binary coalescence literature, the two synthetic stream pertaining to the two polarizations were always a by-product of the MLR analysis of the multi-detector analysis. In this work, for the first time, the authors have derived the synthetic data streams using the matching filtering idea applied to the network combined with the singular-value-decomposition technique applied to the network SNR vector.

Then, the network LLR naturally emerges as the sum of the LLR of the single synthetic stream LLR. The MLR over the new parameters namely the two amplitudes and the two phases is a straightforward task. We further, demonstrate that the dominant polarization plane naturally emerges out of the SVD of the SNR vector.

Connecting this work to the existing literature; namely [8] and [10], we explicitly show that the two synthetic

[10] Hypothetically we take Pune, India as the location for the detector in India.

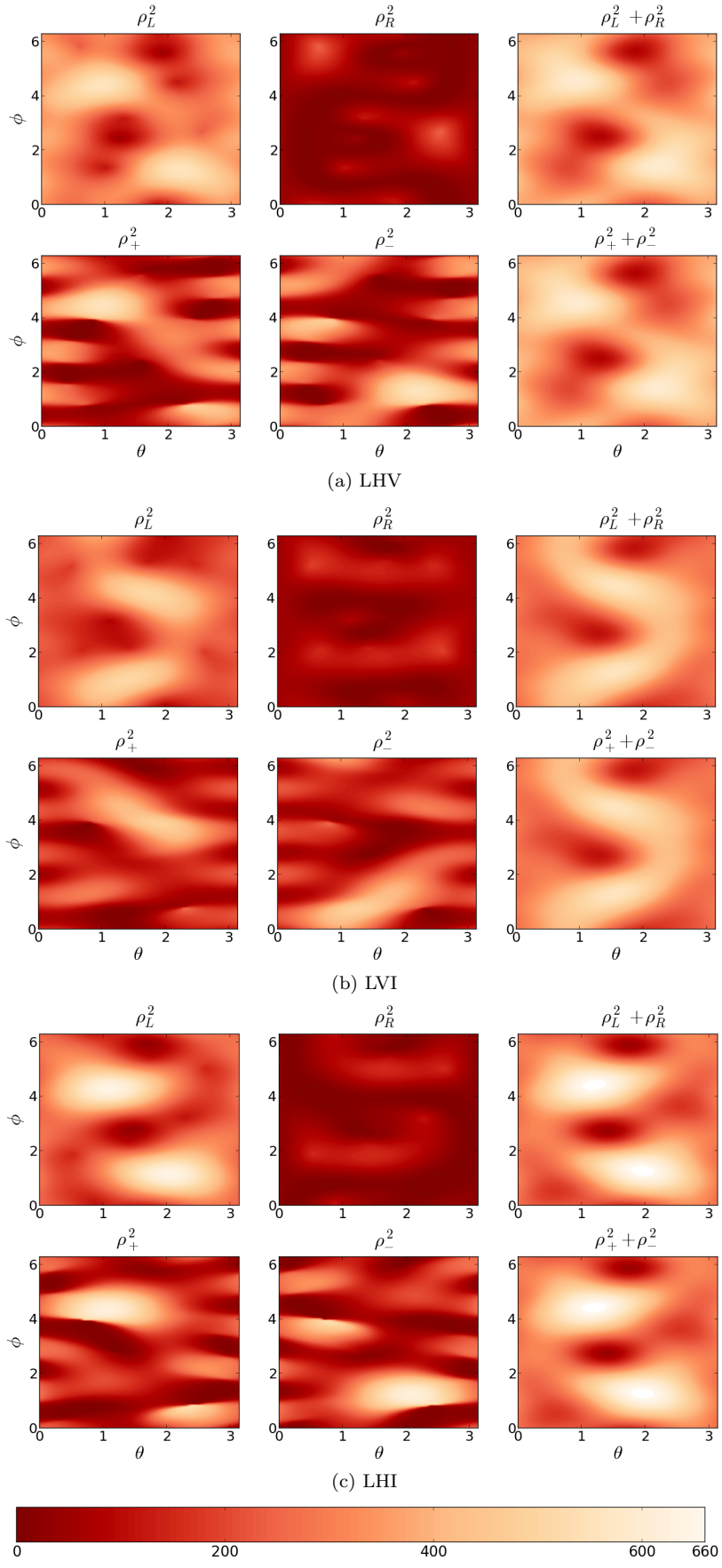

(a) LHV

(b) LVI

(c) LHI

FIG. 1: Directional SNR Squares $\boldsymbol{\rho_L^2}$, $\boldsymbol{\rho_R^2}$, $\boldsymbol{\rho_+^2}$, $\boldsymbol{\rho_-^2}$ and $\boldsymbol{\rho_{net}^2}$ for various three network configurations with $m_1, m_2 = 1.4$, $\epsilon = \pi/4,\ \Psi = \pi/4,\ r = 150 MPc.$ with same noise spectral densities for all detectors.

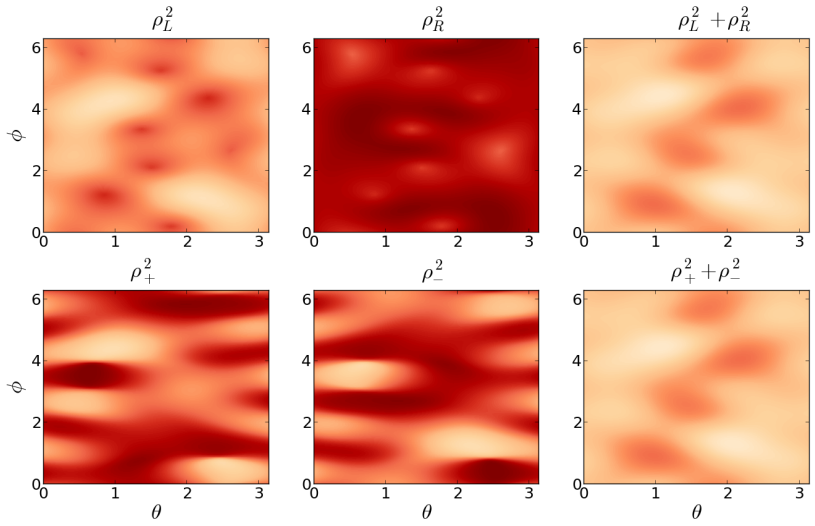

(a) LHVK

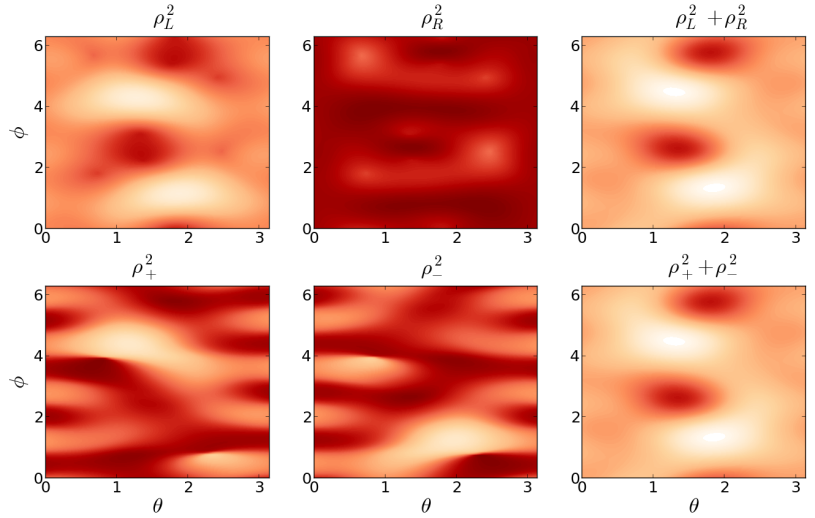

(b) LHVI

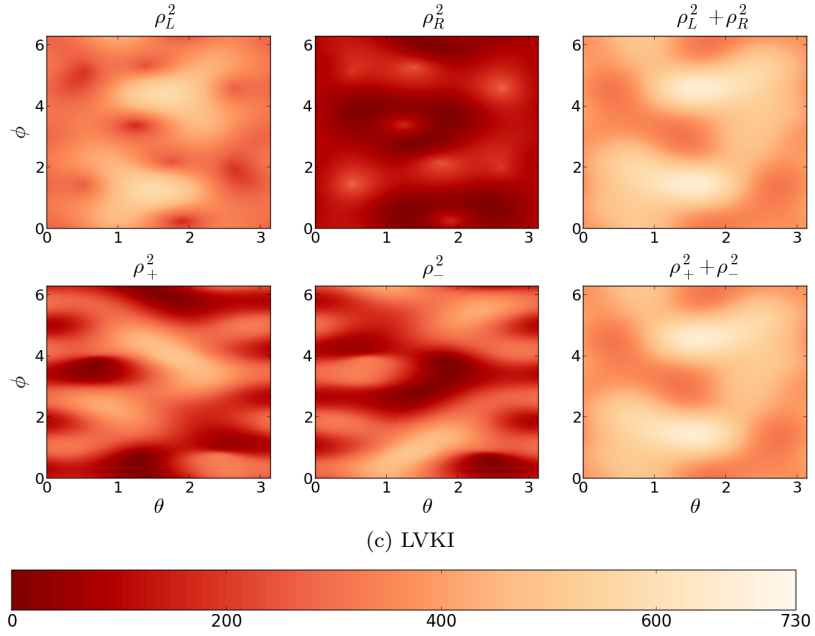

(c) LVKI

FIG. 2: Directional SNR Squares $\boldsymbol{\rho_L^2}$, $\boldsymbol{\rho_R^2}$, $\boldsymbol{\rho_+^2}$, $\boldsymbol{\rho_-^2}$ and $\boldsymbol{\rho_{net}^2}$ for various four detector network configurations with $m_1, m_2 = 1.4$, $\epsilon = \pi/4,\ \Psi = \pi/4,\ r = 150 MPc.$ with same noise spectral densities for all detectors.

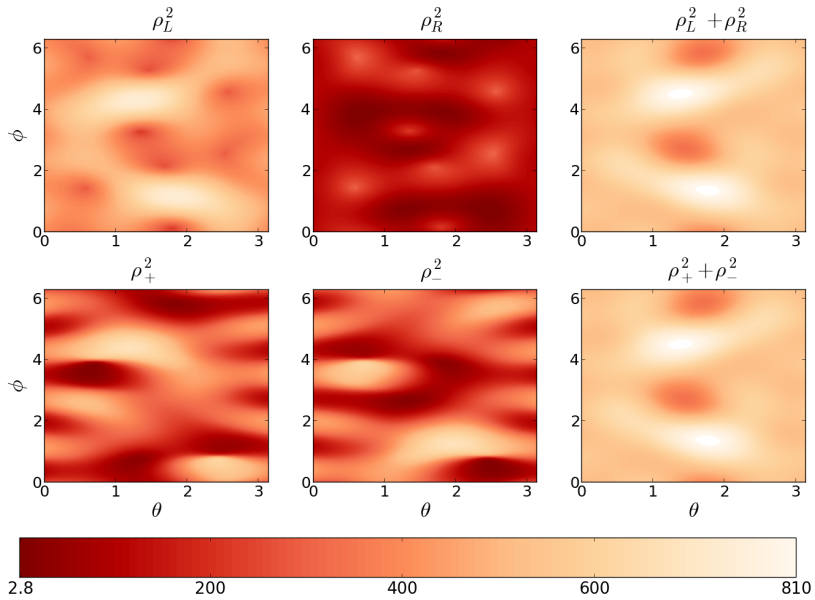

FIG. 3: Directional SNR Squares $\boldsymbol{\rho_L^2}$, $\boldsymbol{\rho_R^2}$, $\boldsymbol{\rho_+^2}$, $\boldsymbol{\rho_-^2}$ and $\boldsymbol{\rho_{net}^2}$ for network LHVKI with $m_1, m_2 = 1.4,\ \epsilon = \pi/4,\ \Psi = \pi/4,$ $r = 150MPc.$ with same noise spectral densities for all detectors.

streams discussed in the earlier works are distinct and they can be related through the network constructs. Though this work is theoretical in nature, it combines all the existing formalisms of the multi-detector pertaining to the compact binary coalescence. We are further investigating the properties of these streams and its possible applications in the inspiraling binary search namely to develop the consistency tests as well as to carry out efficient all-sky search with a global detector network.

VIII. ACKNOWLEDGEMENT

This work is supported by AP's SERC Fast Track Scheme For Young Scientists. HK thanks Albert Einstein Institute, Hannover for hospitality for stay during where part of the manuscript writing was carried out. The authors would like to thank S. Fairhurst, B. S. Santhyaprakash and Gianluca Guidi for useful discussion and helpful comments on this work. The main result of this work is presented in the LIGO-Virgo Scientific Meeting at Hannover, 2013 (LIGO laboratory document number: LIGO-G1301109). This document has been assigned LIGO laboratory document number LIGO-P1300229.

Appendix A: Likelihood Ratio

The network log Likelihood Ratio,

$$\Lambda = \sum_{m=1}^{I} \langle \mathbf{x}_m | \mathbf{s}_m \rangle - \frac{1}{2} \langle \mathbf{s}_m | \mathbf{s}_m \rangle$$

$$= \sum_{m=1}^{I} \ 4\Re \left[\sum_{j=1}^{N} \tilde{\tilde{\mathcal{X}}}_{jm} \tilde{\mathcal{S}}^*_{jm} \right] - 2 \left[\sum_{j=1}^{N} \frac{\left| \tilde{\mathcal{S}}_{jm} \right|^2}{\mathcal{N}_{jm}} \right] . \qquad \text{(A1)}$$

We use Eq.(34) to express the network LLR in terms of $(P_L, P_R, \Phi_L, \Phi_R)$ etc, we get

$$\sum_{m=1}^{I} 4\Re \left[\sum_{j=1}^{N} \tilde{\tilde{\mathcal{X}}}_{jm}\ \tilde{S}^*_{jm} \right] = 4\mathrm{A}_0\mathrm{P}_L\ \Re \left[\sum_{j=1}^{N} \sum_{m=1}^{I} \tilde{\tilde{\mathcal{X}}}_{jm} \mathrm{F}^{DP}_{+m}\ \tilde{h}^*_{0j} e^{-i\Phi_L} \right] + 4\mathrm{A}_0\mathrm{P}_R\ \Re \left[\sum_{j=1}^{N} \sum_{m=1}^{I} \tilde{\tilde{\mathcal{X}}}_{jm} \mathrm{F}^{DP}_{\times m}\ \tilde{h}^*_{0j} e^{-i\Phi_R} \right]$$

$$= \mathrm{A}_0 \left[\mathrm{P}_L \| \mathbf{F}^{'DP}_{+} \| \langle \mathbf{z}_L | \mathbf{h}_0 e^{i\Phi_L} \rangle + \mathrm{P}_R \| \mathbf{F}^{'DP}_{\times} \| \langle \mathbf{z}_R | \mathbf{h}_0 e^{i\Phi_R} \rangle \right] . \qquad \text{(A2)}$$

Eq.(13) and Eq.(16), gives

$$\mathrm{A}_0\mathrm{P}_L \| \mathbf{F}^{'DP}_{+} \| = \boldsymbol{\rho}_L\ , \qquad \mathrm{A}_0\mathrm{P}_R \| \mathbf{F}^{'DP}_{\times} \| = \boldsymbol{\rho}_R\ . \qquad \text{(A3)}$$

Also, from Eq.(7) one can easily show that the second terms in Eq.(A1) is half of network SNR square, $\boldsymbol{\rho}_L^2 + \boldsymbol{\rho}_R^2$. Substituting back in Eq.(A1),

$$2\Lambda = \left[2\boldsymbol{\rho}_L \langle \mathbf{z}_L | \mathbf{h}_0 e^{i\Phi_L} \rangle - \boldsymbol{\rho}_L^2 \right] + \left[2\boldsymbol{\rho}_R \langle \mathbf{z}_R | \mathbf{h}_0 e^{i\Phi_R} \rangle - \boldsymbol{\rho}_R^2 \right] . \qquad \text{(A4)}$$

Appendix B: Relation between old and new extrinsic parameters

MLR is obtained by maximizing network LLR over the four extrinsic parameters, which are the functions of physical parameters, $(\mathrm{A}_0, \phi_a, \epsilon, \Psi)$. As we discussed earlier, the choice of these functions depend on the formalism. But the final results for various approaches will remain same.

The extrinsic parameters used in this paper are,

$$\begin{aligned}
\boldsymbol{\rho}_L &= \mathrm{A}_0 \|\mathbf{F}_+^{DP}\| \sqrt{\left(\frac{1+\cos^2\epsilon}{2}\right)^2 \cos^2 2\chi + \cos^2\epsilon \sin^2 2\chi}, \\
\boldsymbol{\rho}_R &= \mathrm{A}_0 \|\mathbf{F}_2^{DP}\| \sqrt{\left(\frac{1+\cos^2\epsilon}{2}\right)^2 \sin^2 2\chi + \cos^2\epsilon \cos^2 2\chi}, \\
\Phi_L &= \tan^{-1}\left[\tan(2\chi)\ \ \frac{2\cos\epsilon}{1+\cos^2\epsilon}\right] + \phi_a, \\
\Phi_R &= \tan^{-1}\left[-\cot(2\chi)\ \ \frac{2\cos\epsilon}{1+\cos^2\epsilon}\right] + \phi_a. \qquad \text{(B1)}
\end{aligned}$$

In [10], the maximization of LLR is done over a set of derived amplitude parameters,

$$\begin{aligned}
\mathcal{A}_1 &= \mathrm{A}_0 \left[\frac{1+\cos^2\epsilon}{2}\cos\phi_a \cos 2\Psi - \cos\epsilon \sin\phi_a \sin 2\Psi\right], \\
\mathcal{A}_2 &= \mathrm{A}_0 \left[\frac{1+\cos^2\epsilon}{2}\cos\phi_a \sin 2\Psi + \cos\epsilon \sin\phi_a \cos 2\Psi\right], \\
\mathcal{A}_3 &= \mathrm{A}_0 \left[-\frac{1+\cos^2\epsilon}{2}\sin\phi_a \cos 2\Psi - \cos\epsilon \cos\phi_a \sin 2\Psi\right], \\
\mathcal{A}_4 &= \mathrm{A}_0 \left[-\frac{1+\cos^2\epsilon}{2}\sin\phi_a \sin 2\Psi + \cos\epsilon \cos\phi_a \cos 2\Psi\right]. \qquad \text{(B2)}
\end{aligned}$$

These are related to $(\boldsymbol{\rho}_L, \boldsymbol{\rho}_R, \Phi_L, \Phi_R)$ as follows,

$$\begin{aligned}
\boldsymbol{\rho}_L &= \|\mathbf{F}_+'^{DP}\| \left|(\mathcal{A}_1 - i\mathcal{A}_3)\cos\frac{\delta}{2} + (\mathcal{A}_2 - i\mathcal{A}_4)\sin\frac{\delta}{2}\right|, \\
\boldsymbol{\rho}_R &= \|\mathbf{F}_\times'^{DP}\| \left|(\mathcal{A}_2 - i\mathcal{A}_4)\cos\frac{\delta}{2} - (\mathcal{A}_1 - i\mathcal{A}_3)\sin\frac{\delta}{2}\right|, \\
\Phi_L &= arg\left[(\mathcal{A}_1 - i\mathcal{A}_3)\cos\frac{\delta}{2} + (\mathcal{A}_2 - i\mathcal{A}_4)\sin\frac{\delta}{2}\right], \\
\Phi_R &= arg\left[(\mathcal{A}_2 - i\mathcal{A}_4)\cos\frac{\delta}{2} - (\mathcal{A}_1 - i\mathcal{A}_3)\sin\frac{\delta}{2}\right]. \qquad \text{(B3)}
\end{aligned}$$

Appendix C: Likelihood Estimates of Polarization angles

As we discussed earlier, a network of detectors can recover the polarization information of GW. Since $\mathbf{z}_L$ and $\mathbf{z}_R$ are the equivalent detectors of the network, we can obtain the estimates of polarization angles $\hat{\epsilon}$ and $\hat{\Psi}$ in terms of their SNRs.

By using Eq.(13),Eq.(16) and definition of $\Phi_{L,R}$ we define,

$$\begin{aligned}
Y &\equiv \frac{\boldsymbol{\rho}_L \|\mathbf{F}_\times^{DP}\| \mathbf{e}^{i\Phi_L}}{\boldsymbol{\rho}_R \|\mathbf{F}_+^{DP}\| \mathbf{e}^{i\Phi_R}} = \frac{\cos 2\chi\ \frac{1+\cos^2\epsilon}{2} + i \sin 2\chi\ \cos\epsilon}{\sin 2\chi\ \frac{1+\cos^2\epsilon}{2} - i\cos 2\chi\ \cos\epsilon} \\
&= i\frac{T^*_{2+2}(\chi,\epsilon,0) + T^*_{2-2}(\chi,\epsilon,0)}{T^*_{2+2}(\chi,\epsilon,0) - T^*_{2-2}(\chi,\epsilon,0)}, \qquad \text{(C1)}
\end{aligned}$$

This implies,

$$\frac{T_{2-2}(\chi,\epsilon,0)}{T_{2+2}(\chi,\epsilon,0)} = \frac{iY^* - 1}{iY^* + 1}. \qquad \text{(C2)}$$

Then polarization angles can be expressed in terms of Y as follows.

$$\begin{aligned}
\cos 4\Psi &= \cos\left[arg\left(\frac{T_{2-2}}{T_{2+2}}\right) + \delta\right] \\
&= \cos\left[arg\left(\frac{iY^* - 1}{iY^* + 1}\right) + \delta\right], \qquad \text{(C3)}
\end{aligned}$$

and

$$\cos\epsilon = \frac{1 - \sqrt{\left|\frac{T_{2-2}}{T_{2+2}}\right|}}{1 + \sqrt{\left|\frac{T_{2-2}}{T_{2+2}}\right|}} = \frac{1 - \sqrt{\left|\frac{iY^*-1}{iY^*+1}\right|}}{1 + \sqrt{\left|\frac{iY^*-1}{iY^*+1}\right|}}. \qquad \text{(C4)}$$

However, when the noise is present $\boldsymbol{\rho}_L, \boldsymbol{\rho}_R, \Phi_L, \Phi_R$ are estimated using MLR approach. Then using Eq.(C1), Y is constructed out of $\hat{\boldsymbol{\rho}}_L, \hat{\boldsymbol{\rho}}_R, \hat{\Phi}_L, \hat{\Phi}_R$ estimates. Thus $(\hat{\epsilon}, \hat{\Psi})$ is obtained by Eq.(C3) and Eq.(C4), with newly constructed Y.

[1] G. M. Harry (LIGO Scientific Collaboration), Class.Quant.Grav. **27**, 084006 (2010).

[2] The Virgo Collaboration, Tech. Rep. VIR-0027A-09, Virgo Collaboration (2009), URL `https://tds.ego-gw.it/ql/?c=6589`.

[3] K. Somiya (KAGRA Collaboration), Class.Quant.Grav. **29**, 124007 (2012), 1111.7185.

[4] J. Abadie et al. (LIGO Scientific Collaboration, Virgo Collaboration), Class.Quant.Grav. **27**, 173001 (2010), 1003.2480.

[5] B. J. Owen and B. S. Sathyaprakash, Phys. Rev. D **60**, 022002 (1999), URL `http://link.aps.org/doi/10.1103/PhysRevD.60.022002`.

[6] B. S. Sathyaprakash and S. V. Dhurandhar, Phys. Rev. D **44**, 3819 (1991), URL `http://link.aps.org/doi/10.1103/PhysRevD.44.3819`.

[7] S. Fairhurst, New J.Phys. **11**, 123006 (2009), 0908.2356.

[8] A. Pai, S. Dhurandhar, and S. Bose, Phys. Rev. D

64, 042004 (2001), URL http://link.aps.org/doi/10.1103/PhysRevD.64.042004.

[9] L. S. Finn, Phys. Rev. D **63**, 102001 (2001), URL http://link.aps.org/doi/10.1103/PhysRevD.63.102001.

[10] I. W. Harry and S. Fairhurst, Phys. Rev. D **83**, 084002 (2011), URL http://link.aps.org/doi/10.1103/PhysRevD.83.084002.

[11] P. Jaranowski, A. Królak, and B. F. Schutz, Phys. Rev. D **58**, 063001 (1998), URL http://link.aps.org/doi/10.1103/PhysRevD.58.063001.

[12] C. Cutler and B. F. Schutz, Phys. Rev. D **72**, 063006 (2005), URL http://link.aps.org/doi/10.1103/PhysRevD.72.063006.

[13] S. Klimenko, S. Mohanty, M. Rakhmanov, and G. Mitselmakher, Phys. Rev. D **72**, 122002 (2005), URL http://link.aps.org/doi/10.1103/PhysRevD.72.122002.

[14] J. Sylvestre, Phys. Rev. D **68**, 102005 (2003), URL http://link.aps.org/doi/10.1103/PhysRevD.68.102005.

[15] A. Pai, E. Chassande-Mottin, and O. Rabaste, Phys. Rev. D **77**, 062005 (2008), URL http://link.aps.org/doi/10.1103/PhysRevD.77.062005.

[16] D. Keppel, ArXiv e-prints (2013), 1307.4158.

[17] K. G. Arun, B. R. Iyer, B. S. Sathyaprakash, and P. A. Sundararajan, Phys. Rev. D **71**, 084008 (2005), URL http://link.aps.org/doi/10.1103/PhysRevD.71.084008.

[18] B. F. Schutz, ArXiv e-prints (1997), gr-qc/9710080.

[19] Y. Gürsel and M. Tinto, Phys. Rev. D **40**, 3884 (1989), URL http://link.aps.org/doi/10.1103/PhysRevD.40.3884.

[20] *The very large telescope interferometer*, URL www.eso.org/paranal/telescopes/vlti/.

[21] *Very-long-baseline interferometry*, URL en.wikipedia.org/wiki/Very-long-baseline_interferometry.

[22] S. Dhurandhar and M. Tinto, MNRAS **234**, 663 (1998).

[23] M. Maggiore, *Gravitational Waves: Volume 1: Theory and Experiments* (Oxford University Press, USA, 2008).

[24] P. Ajith, Phys. Rev. D **84**, 084037 (2011), URL http://link.aps.org/doi/10.1103/PhysRevD.84.084037.